

AD-A056 261

AERONAUTICAL RESEARCH LABS MELBOURNE (AUSTRALIA)
AN ULTRASONIC PULSE-HEIGHT DIFFERENCE METHOD OF RECORDING CRACK--ETC(U)
SEP 77 W J POLLOCK, A J FARRELL

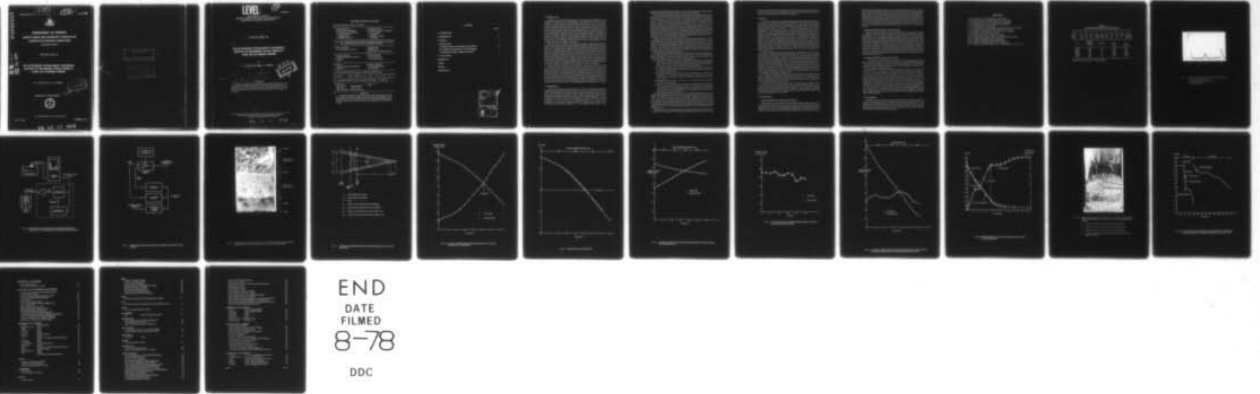
F/G 11/6

UNCLASSIFIED

ARL/MAT.120

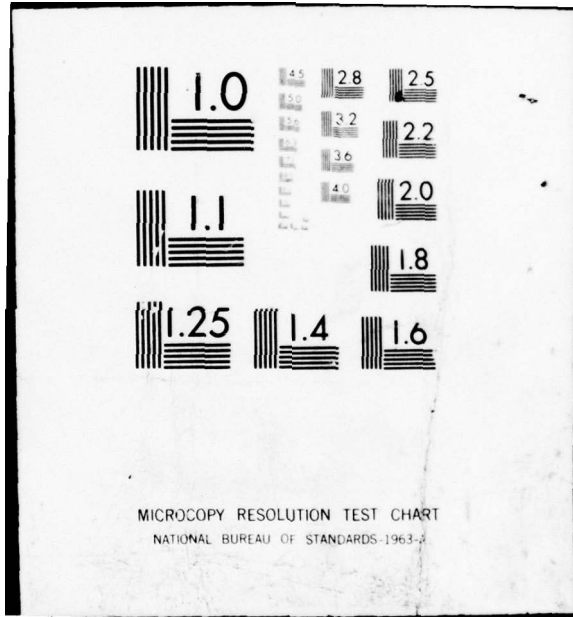
NL

| OF |
AD
A056261



END
DATE
FILMED
8-78

DDC



MICROCOPY RESOLUTION TEST CHART
NATIONAL BUREAU OF STANDARDS-1963-A

AD A 056261

ARL-Mat-Note-120

LEVEL III

12

AR-000-954



DEPARTMENT OF DEFENCE
DEFENCE SCIENCE AND TECHNOLOGY ORGANISATION
AERONAUTICAL RESEARCH LABORATORIES
MELBOURNE, VICTORIA

MATERIALS NOTE 120

AN ULTRASONIC PULSE-HEIGHT DIFFERENCE
METHOD OF RECORDING CRACK GROWTH
OVER AN EXTENDED PERIOD

W. J. POLLOCK and A. J. FARRELL

D D C
RECEIVED
JUL 18 1978
F

Approved for Public Release



© COMMONWEALTH OF AUSTRALIA 1977

COPY No 18

SEPTEMBER 1977

78 07 17 039

AD No. —
DDC FILE COPY

APPROVED
FOR PUBLIC RELEASE

THE UNITED STATES NATIONAL
TECHNICAL INFORMATION SERVICE
IS AUTHORIZED TO
REPRODUCE AND SELL THIS REPORT

LEVEL

12

AR-000-854

DEPARTMENT OF DEFENCE
DEFENCE SCIENCE AND TECHNOLOGY ORGANISATION
AERONAUTICAL RESEARCH LABORATORIES

9 MATERIALS NOTE 120

6

AN ULTRASONIC PULSE-HEIGHT DIFFERENCE METHOD OF RECORDING CRACK GROWTH OVER AN EXTENDED PERIOD.

by

10 W. J. POLLOCK and A. J. FARRELL

DDC
RECEIVED
JUL 18 1978
F

11 Sep 77 / 12 27p

14 ARL/MAT. 120

SUMMARY

A method for recording slow crack growth, using a conventional ultrasonic tester and chart recorder, is described. The problems caused by changes in the measuring system over long periods were overcome by relating crack growth to the amplitude difference between the crack reflection and a reference reflection. Some applications of the technique are described.

POSTAL ADDRESS: Chief Superintendent, Aeronautical Research Laboratories,
Box 4331, P.O., Melbourne, Victoria, 3001, Australia.

78 07 17 039

008 650

JOB

DOCUMENT CONTROL DATA SHEET

Security classification of this page: Unclassified

- | | |
|---|--|
| <p>1. Document Numbers</p> <p>(a) AR Number: AR-000-854</p> <p>(b) Document Series and Number:
Materials Note 120</p> <p>(c) Report Number:
ARL/Mat. Note 120 ✓</p> | <p>2. Security Classification</p> <p>(a) Complete document: Unclassified</p> <p>(b) Title in isolation:
Unclassified</p> <p>(c) Summary in isolation:
Unclassified</p> |
|---|--|

3. Title: AN ULTRASONIC PULSE-HEIGHT DIFFERENCE METHOD OF RECORDING CRACK GROWTH OVER AN EXTENDED PERIOD ✓

- | | |
|---|---|
| <p>4. Personal Author(s):
W. J. Pollock and A. J. Farrell</p> | <p>5. Document Date:
September, 1977 ✓</p> <p>6. Type of Report and Period Covered:</p> |
|---|---|

- | | |
|--|---|
| <p>7. Corporate Author(s):
Aeronautical Research Laboratories</p> <p>9. Cost Code:
35 1610</p> | <p>8. Reference Numbers</p> <p>(a) Task: AIR 72/8</p> <p>(b) Sponsoring Agency:</p> |
|--|---|

- | | |
|--|---|
| <p>10. Imprint
Aeronautical Research Laboratories,
Melbourne</p> | <p>11. Computer Program(s)
(Title(s) and language(s)):
Not Applicable</p> |
|--|---|

12. Release Limitations (of the document): Approved for Public Release

12-0. Overseas:	No.	P.R.	I	A	B	C	D	E
-----------------	-----	------	---	---	---	---	---	---

13. Announcement Limitations (of the information on this page): No Limitation

- | | |
|---|-----------------------------------|
| <p>14. Descriptors:</p> <p>Stress corrosion Crack propagation</p> <p>D6AC steel Ultrasonic tests</p> <p>High strength steels Pulse echo technique</p> | <p>15. Cosati Codes:
1113</p> |
|---|-----------------------------------|

16. **ABSTRACT**

A method for recording slow crack growth, using a conventional ultrasonic tester and chart recorder, is described. The problems caused by changes in the measuring system over long periods were overcome by relating crack growth to the amplitude difference between the crack reflection and a reference reflection. Some applications of the technique are described.

CONTENTS

	Page No.
1. INTRODUCTION	1
2. EXPERIMENTAL	1-3
3. RESULTS	3
4. APPLICATIONS	3
4.1 Incubation Periods due to Reduction in Stress Intensity	3-4
4.2 Accelerated Crack Growth due to Crack-Front Bowing	4
4.3 Incubation Periods due to Changes in Environment	4
5. CONCLUSIONS	4
REFERENCES	
TABLES	
FIGURES	
DISTRIBUTION	

ACCESSION for	
NTIS	White Section <input checked="" type="checkbox"/>
DDC	B-1 Section <input type="checkbox"/>
UNANNOUNCED	<input type="checkbox"/>
JUSTIFICATION	
BY	
DISTRIBUTION/AVAILABILITY CODES	
D.	and/or SPECIAL
A	

1. INTRODUCTION

Application of fracture mechanics principles (ref. 1) has enabled critical defect sizes to be estimated in critical components of high performance structures provided a stress analysis of the component is available and the fracture toughness of the material is known. In an effort to investigate how long a given defect will take to reach this critical level, a number of techniques have been developed to monitor crack-growth rates in small precracked test specimens. These methods include (a) optical monitoring at the specimen surface, (b) measuring the change in crack-opening-displacement (COD), (c) electrical potential methods, (d) acoustic emission, and (e) ultrasonic pulse-echo techniques. The choice of crack-measuring technique is determined by (a) type of information sought, (b) method of specimen loading, (c) visibility, accessibility and geometry of the crack under study, and (d) specimen geometry. Acoustic emission, electrical potential and COD measurements provide information from which mean cracking rates across the crack front can be calculated, whereas optical and ultrasonic measurements give more localised information on the progress of cracking.

Since stress-corrosion cracking is often controlled by processes occurring in the plane-strain region near the specimen centre, the ultrasonic pulse-echo technique is ideally suited for this type of study. If the ultrasonic probe is aligned normal to the crack plane, a typical trace on the tester screen shows a transmitted pulse, a reflection from the crack and a reflection from the back-wall (fig. 1). In one method of operation (refs. 2-5), the ultrasonic probe is adjusted such that the amplitude of the reflected signal from the crack is just less than some preset level. Once cracking starts, the (crack-peak) amplitude exceeds this preset level and the probe is moved a given distance ahead of the crack to wait for the signal to reach the preset level. In instances where the probe cannot be moved readily (e.g. in a vacuum system or enclosed space), a second method has been developed in which the probe is cemented in position and crack growth determined from the change in amplitude of the reflected signal from the crack (refs. 6-9). Precalibration in this instance was achieved by extending a slot with a thin saw to simulate crack growth.

Crack growth during stress-corrosion cracking (SCC) is often so slow that it takes several days to extend the crack a measurable amount. Under these circumstances, drift in the ultrasonic tester electronics becomes a problem and may seriously impair the sensitivity of the method. The present work describes a new mode of operation which distinguishes between crack growth and long-term drift effects. The method makes use of the changes in amplitude of the reflected signals from both the crack and the back-wall of the specimen during cracking. Since the amplitude of the crack-peak increases and the back-wall peak decreases during cracking, the difference (ΔH) provides a sensitive measure of the cracking process. Long-term drift effects due to changes in temperature, probe pressure and electronic instabilities will cause the amplitudes of both peaks to move in phase and hence they can be readily distinguished from changes due to crack growth.

2. EXPERIMENTAL

Following the experience of other workers (refs. 2, 3, 9), the ultrasonic technique was designed to operate with 23 mm thick side-grooved 1-T WOL specimens (fig. 2A) (ref. 10) using either D6AC or SD19 steel. Heat-treatment for D6AC steel used in this study involved austenitising for 30 minutes at 930°C, quenching to 'Ausbay' at 520°C and holding for 30 minutes, further quenching into circulating hot oil at 60°C, cooling to 25°C and double-tempering for 1+1 hours at either 290°C or 565°C. SD19 steel was austenitised for 1 hour at 860°C, quenched into circulating hot oil at 52°C, cooled to 25°C and double-tempered for 1+1 hours at 400°C. Composition, tensile and fracture toughness properties are listed in Table 1. Specimens were machined with cracks aligned in either the T-L or L-T orientations (fig. 3). Prior to SCC,

specimens were fatigue precracked at 10 Hz in air at 25°C and cracks extended to approximately 5 mm from the notch with the stress intensity varying from 2 to 20 MPa m^{1/2}.

The crack was monitored ultrasonically with a Krautkramer ultrasonic detector coupled in turn to each of four 6 mm diameter, 12 MHz probes mounted on the specimen with their centres located at intervals of 3.25 mm in the direction of cracking (fig. 2B). Apiezon L vacuum grease was used as couplant and each probe was held on the specimen surface by a compression spring loaded by a bolt. With each probe monitoring approximately 3 mm of crack growth, it was possible to register 12 mm crack growth before resetting the probes. As shown in fig. 4, the demodulated signal from the ultrasonic tester, i.e. the signal displayed on the tester screen, is gated and the amplitude of the gated signal sampled by a sample-and-hold (SAH) circuit. In the sample pulse-switching circuit (fig. 5), two sets of sampling pulses are generated, one set being adjusted to coincide with the crack pulse and the other to coincide with the back-wall pulse. At ten second intervals, the sampling pulse is switched to the SAH sampling pulse input, so that the amplitude of the crack pulse and the back-wall pulse appear alternately on the chart recorder. A detailed description of the circuits appears in reference 11.

Calibration of the ultrasonics was achieved by stress-corroding the specimen at constant load and monitoring the change in crack length using both the ultrasonic tester and a linear variable differential transducer (LVDT) mounted on the top face of the specimen to monitor changes in the crack-opening-displacement (COD). Provided the whole crack front moves at the same rate, crack growth rates calculated from the LVDT output can be used to calibrate the ultrasonics. This condition was achieved by positioning the first ultrasonic probe well ahead of the crack front prior to SCC such that steady-state cracking at constant load was reached by the time the crack front crossed the ultrasonic beam.

Since the theoretical compliance C (change in COD/load P) is known over the full length of the 1-T WOL specimen (ref. 10), then SCC crack-growth data can be readily calculated from COD measurements by adopting the following iterative procedure, provided the initial crack length of the specimen prior to stress-corrosion cracking is known:

- (a) After the SCC experiment is terminated, the specimen is broken open and the fracture surface used to measure the mean crack length from the load line prior to the commencement of SCC. This value is easily measured as the fracture surface of the fatigue pre-crack is usually much smoother than the SCC fracture surface (fig. 6).
- (b) The change in COD (V_{1f}) during application of load P prior to SCC is measured and converted to an equivalent value at the load line (V_{2f}) using similar triangles and knowing the initial crack length a (fig. 7).
- (c) By continually monitoring the change in COD on a chart recorder, a new COD (V_{1f}) is obtained after a small increment of SCC at constant load P . If the new crack length is assumed to be $a + da$, then the new COD at the load line is calculated by similar triangles to be V_{2f} (fig. 7).
- (d) Dividing the change in COD at the load line ($V_{2f} - V_{2f}$) by the load P gives the change in compliance (ΔC) during SCC.
- (e) If the mean crack length during SCC is taken as $a + da/2$ and the theoretical rate of change in compliance with crack length is known (ref. 10) $((dC/da)_{\text{theor}})$, then dividing ΔC by $(dC/da)_{\text{theor}}$ gives a better approximation of the estimated value da . Substitution of da back into step (c) and repeating iteratively gives continually better estimates of the stress-corrosion crack-growth increment.

The above procedure was then repeated for successive selected increments of stress-corrosion crack growth throughout the life of the specimen. Provided crack-growth rates did not vary rapidly, crack growth increments of 1 mm were adequate to quantify the cracking kinetics. Errors of less than 10% were found when the sum of these calculated values of crack-growth were compared with values experimentally measured from the fracture surface (ref. 12). These rates were then used to calibrate the ultrasonic data using calculated ΔH values. In order to standardise the ultrasonic output, the gain on the Krautkramer was adjusted to give a signal amplitude of 0.50 ± 0.05 volts when the amplitude of both the crack and back-wall peaks were equal ('cross-over').

Calibration runs were performed using D6AC steel specimens tempered to 290°C and stress-corroded in the L-T orientation at low-medium stress intensities in distilled water at 25°C. Stress-

corrosion cracking with this heat treatment of steel was rapid ($1 \mu\text{m}/\text{sec}$) and bowing of the crack front was not observed. The water was applied in the form of a continual drip in the region of the crack so that the ultrasonic probes were kept dry throughout.

3. RESULTS

A typical trace of the change in amplitude of the crack and back-wall peaks during SCC is shown in fig. 8. Using the known cracking rate from LVDT data, the change in ΔH with increasing crack length was determined (fig. 9). It was noted that the crack-growth rate often remained constant during its progress across each of the probes. In the region of the 'cross-over' of the crack and back-wall peaks, ΔH was found to vary linearly with crack length over a distance of approximately 1 mm. The technique can still be used, but with reduced sensitivity, over the remainder of the probe range. Repetition of the probe calibration revealed that the rate of increase in crack-peak amplitude did not always match the rate of decrease in back-wall peak amplitude (fig. 10). The reason for this behaviour was not investigated but its effect was to increase the scatter in the measured ultrasonic sensitivity. A mean value for $d(\Delta H)/da$ was obtained from 13 independent experiments and found to be 0.55 volt/mm, with a standard deviation of 0.16 volt/mm. Although the reproducibility of the calibration appears poor, it compares favourably with the scatter obtained in measuring stress-corrosion crack-growth rates in high strength steels—scatter bands incorporating ten-fold variations are not uncommon in the stress-corrosion cracking of D6AC steel (ref. 13). A similar sensitivity was found when the calibration was carried out with D6AC steel tempered to 565°C , where the stress-corrosion rates were 100 times slower.

In short-term experiments (a few minutes), changes in crack length of 0.1 mm could be readily detected. The effect of long-term drift in amplitude of both the crack and back-wall peaks is shown in fig. 11 for a stationary crack. The results showed that, if estimations of crack growth were made solely from changes in amplitude of the crack-peak, then the ultrasonics could not positively determine cracking unless increments of crack growth exceeded 1 mm. This value is close to the accuracy obtained by Blau (ref. 5) in which crack-growth measurements based on the height of the crack-peak amplitude were taken over the course of several days during SCC of an aluminium alloy. Since the amplitudes of both the crack and back-wall peaks moved in phase, the effects of long-term drift could be largely eliminated through calculation of ΔH , thereby enabling crack extensions of 0.15 mm to be positively identified over a period of several days. Factors which affected long-term drift of the ultrasonics included temperature, mains voltage supply variations and creep in the coupling grease.

The success of the technique is dependent on minimising the scatter of the ultrasonic beam when it is reflected from the fracture surface back to the transducer. This condition was less likely to be satisfied with rough fracture surfaces (region A, fig. 6), hence it was not surprising to find the amplitude behaviour of the crack-peak becoming erratic when some specimens were stress-corroded at high stress intensity (fig. 12).

In some instances at low stress intensity, however, it was found that, in the region of cracking after the 'cross-over', the amplitude of the crack-peak suddenly stopped increasing or even decreased with increasing crack length. When such behaviour occurred, information regarding cracking was lost since the precalibrated ultrasonic sensitivity no longer applied. Consequently, the best range over which sensitive experiments should be conducted is in the vicinity of, and immediately preceding, the 'cross-over' point.

4. APPLICATIONS

4.1 Incubation Periods due to Reduction in Stress Intensity

Measurements of change in COD during SCC provide crack-growth data averaged over the full width of the crack front. Previous work (ref. 14) using the COD technique showed that a propagating stress-corrosion crack experienced an incubation period when the applied load was partially removed. The results of similar experiments using D6AC steel specimens tempered to 290°C and stress-corroded in the L-T orientation in distilled water at 25°C are shown in fig. 13.

Whereas LVDT data suggested that a drop in stress intensity introduced a short period during which crack growth slowed or stopped, ultrasonic monitoring of the crack indicated that propagation continued at the specimen centre. If the rate of crack growth across the full width of the ultrasonic beam (~ 3 mm) at the specimen centre is assumed to be uniform, then it appeared that the crack grew by approximately 0.2 mm at the specimen centre before any change in COD was registered, for both load reductions cited (fig. 13). If it is assumed that little crack growth occurred near the specimen edges during this period, then the mean crack growth across the full crack front would be substantially less than 0.2 mm and the lack of response of the LVDT may be partly due to resolution limitations of the LVDT technique ($\pm 2 \times 10^{-3}$ volts = 0.05 mm crack growth).

4.2 Accelerated Crack Growth due to Crack-Front Bowing

During stress-corrosion cracking of steels and, more particularly, of aluminium alloys, there is a tendency for curved crack fronts to develop. A side-grooved 1-T WOL specimen of D6AC steel tempered to 565°C was fatigue precracked and stress-corroded in the L-T orientation in distilled water at 25°C. Cracking was monitored both ultrasonically and with a LVDT. Three ultrasonic probes were used to monitor cracking and the mean rate, as calculated from LVDT data, for the period during which the crack was monitored by each probe was 0.011, 0.013 and 0.013 $\mu\text{m}/\text{sec}$, respectively. The ultrasonic data for the first and third probes produced rates which agreed substantially with COD measurements, however the cracking rate during the period when the second probe was operational appeared to be almost treble the rate predicted by COD data. This anomaly can be explained by the fact that oxidation markings on the fracture surface (fig. 14) suggest that crack-front bowing developed during the period when the second probe was operating, thus confirming that cracking occurred faster at the centre than near the edges during this short period.

4.3 Incubation Periods due to Changes in Environment

Stress-corrosion cracking in pure gas environments is most easily studied using self-loaded specimens in a vacuum system into which the gas is admitted. The COD at the load line is then constant and ultrasonic monitoring of crack growth complements optical measurements at the specimen surface. With steel specimens, however, the latter technique is not reliable due to difficulties in optically resolving the crack tip.

A bolt-loaded 1-T WOL specimen of D6AC steel tempered to 565°C, was stress-corroded at 80 MPa $\text{m}^{\frac{1}{2}}$ in the T-L orientation in water vapour and water-vapour/oxygen mixtures at 22°C (ref. 15). The changes observed in ΔH during cracking are shown in fig. 15. Addition of 6.5 Pa oxygen to 1.9 kPa water vapour stopped the crack for 8 hours before propagation recommenced. When the oxygen partial pressure was increased by 0.2 kPa, the crack either stopped or slowed down for about one day before continuing to propagate at a constant rate. A similar experiment with SD19 steel (ref. 15) showed that a crack, which had previously been propagating at a stress intensity of 40 MPa $\text{m}^{\frac{1}{2}}$ in 1.4 kPa water vapour at 22°C, stopped for 48 hours after 0.101 MPa (1 atmosphere) air was added and the relative humidity subsequently increased to 100% (fig. 16). After this incubation period, crack propagation resumed at a rate 10^{-3} times slower than in the pure water-vapour environment. In both the experiments cited, optical monitoring of the crack front and fractographic examination confirmed the ultrasonic results obtained. However, the current ultrasonic method gave more immediate indications of when cracking started again.

5. CONCLUSIONS

The difference mode of operation of the ultrasonic pulse-echo technique has been demonstrated to be particularly useful in long-term experiments where instrument drift has to be distinguished from changes due to crack growth. It has also been shown that the use of a single crack-growth measuring technique can sometimes inadequately define the cracking kinetics. Information derived using the current ultrasonic pulse-echo technique can greatly supplement data obtained from optical and COD measurements.

REFERENCES

1. G. R. Irwin and A. A. Wells, *Metall. Rev.* **10**, 223 (1965).
2. W. G. Clark Jr. and L. J. Ceschini, *Mater. Eval.*, **27**, 180 (1969).
3. F. Jeglic, P. Niessen and D. J. Burns, *Exp. Mech.*, **11**, 82 (1969).
4. E. H. Andrews and G. M. Levy, *J. Mater. Sci.*, **6**, 1093 (1971).
5. P. Blau, *Metall. Trans.*, **7A**, 463 (1976).
6. C. E. Lautzenheiser, A. R. Whiting and R. E. Wylie, *Mater. Eval.*, **24**, 241 (1966).
7. C. Terras and C. Janssen, *Mem. Sci. Rev. Metall.*, **67**, 117 (1970).
8. R. F. Lumb and P. Winship, *Met. Constr. Br. Weld. J.*, **3**, 135 (1971).
9. W. G. Clark Jr., *Mater. Eval.*, **25**, 185 (1967).
10. S. R. Novak and S. T. Rolfe, *J. Mater.*, **4**, 701 (1969).
11. A. J. Farrell and P. Ferrarotto, *ARL Instruments Tech. Memo.* 70, (1974).
12. W. J. Pollock, *ARL Materials Note* (in preparation).
13. W. J. Pollock, *ARL Materials Report* (in preparation).
14. D. L. Dull and L. Raymond, *Metall. Trans.*, **3**, 2943 (1972).
15. W. J. Pollock, 3rd Tewksbury Symposium on Fracture, Melbourne, June 1974, 141.

TABLE 1
Composition and Properties of D6AC and SD19 Steels

Wt. %	C	Mn	Si	P	S	Cr	Ni	Mo	V	Fe
D6AC	0.45	0.75	0.22	0.004	0.005	1.10	0.67	1.00	0.090	remainder
SD19	0.41	0.68	0.25	<0.04	<0.04	1.06	0.11	0.21	—	remainder

Steel	Tempering Temperature (°C)	Orientation	UTS (MPa)	K _{1c} (MPam ^{1/2})
D6AC	290	TL	1860	50-65
D6AC	290	LT	1860	62*
D6AC	565	TL	1600	90-99
D6AC	565	LT	1600	98-108
SD19	400	TL	1310	48*

* Estimated using 23 mm thick 1-T WOL specimens.

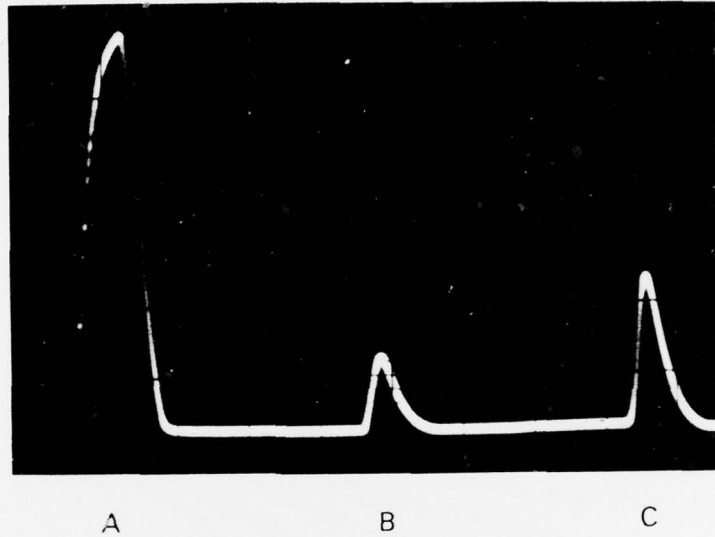


FIG. 1 TYPICAL ULTRASONIC TESTER SCREEN DISPLAY
A: The initial transmitted pulse
B: The pulse reflected from the crack
C: The back-wall echo.

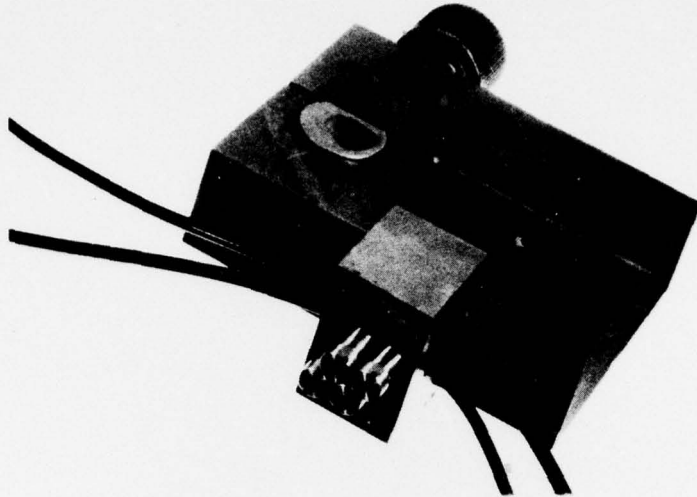


FIG. 2A MODIFIED WOL SPECIMEN WITH ULTRASONIC PROBE ATTACHMENT.

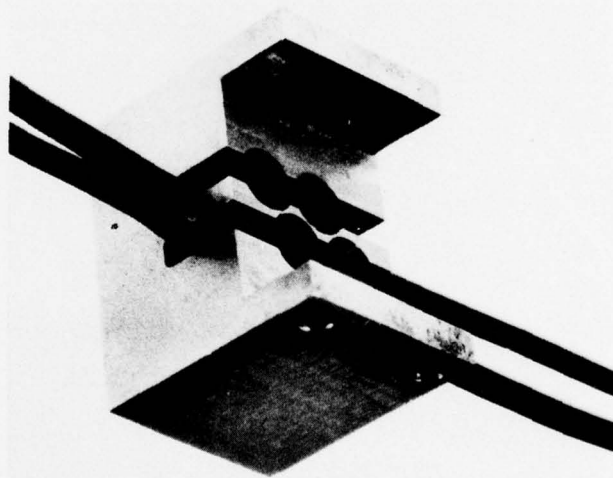


FIG. 2B ULTRASONIC PROBE HOLDER.

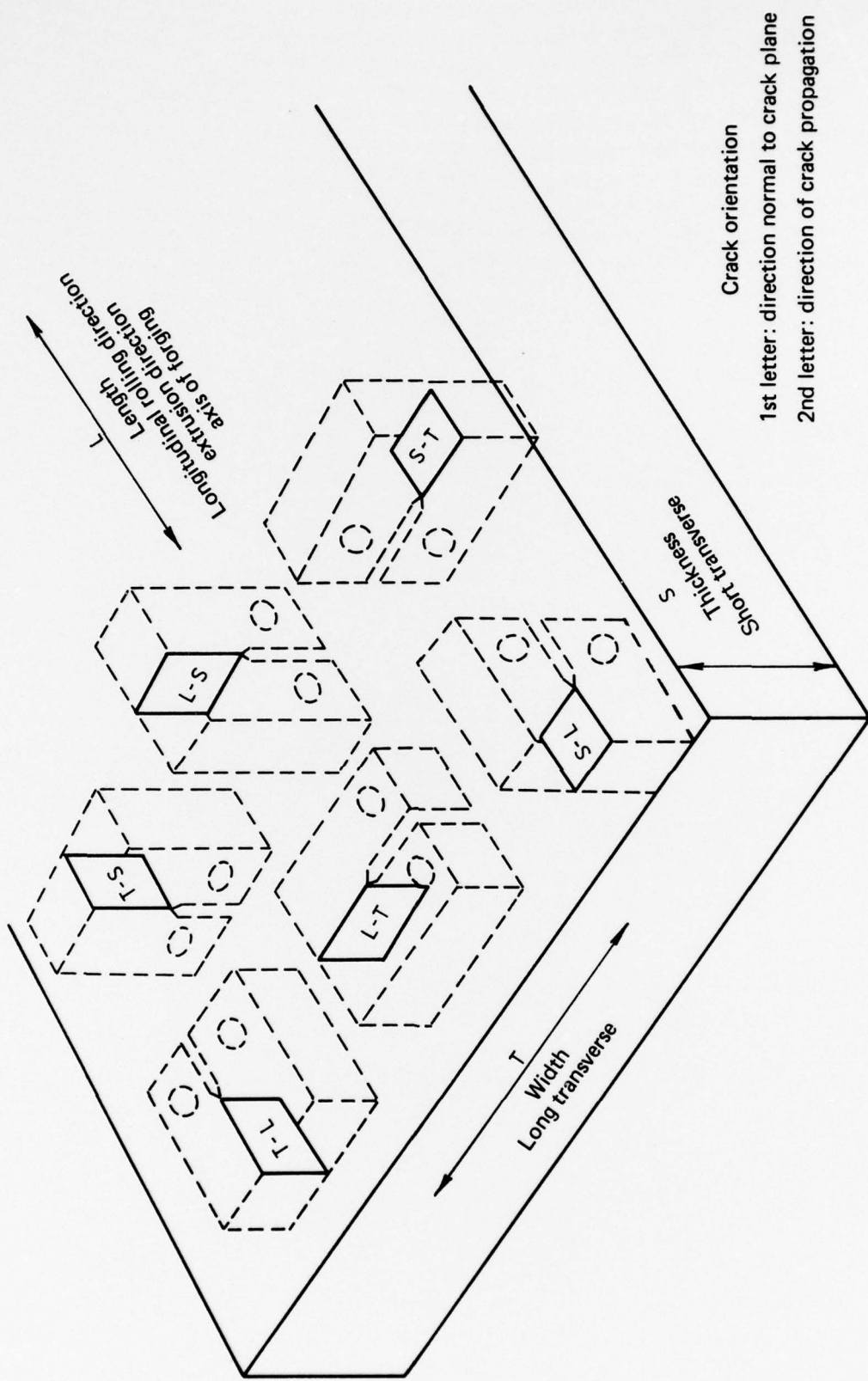


FIG. 3 FRACTURE SPECIMEN ORIENTATIONS.

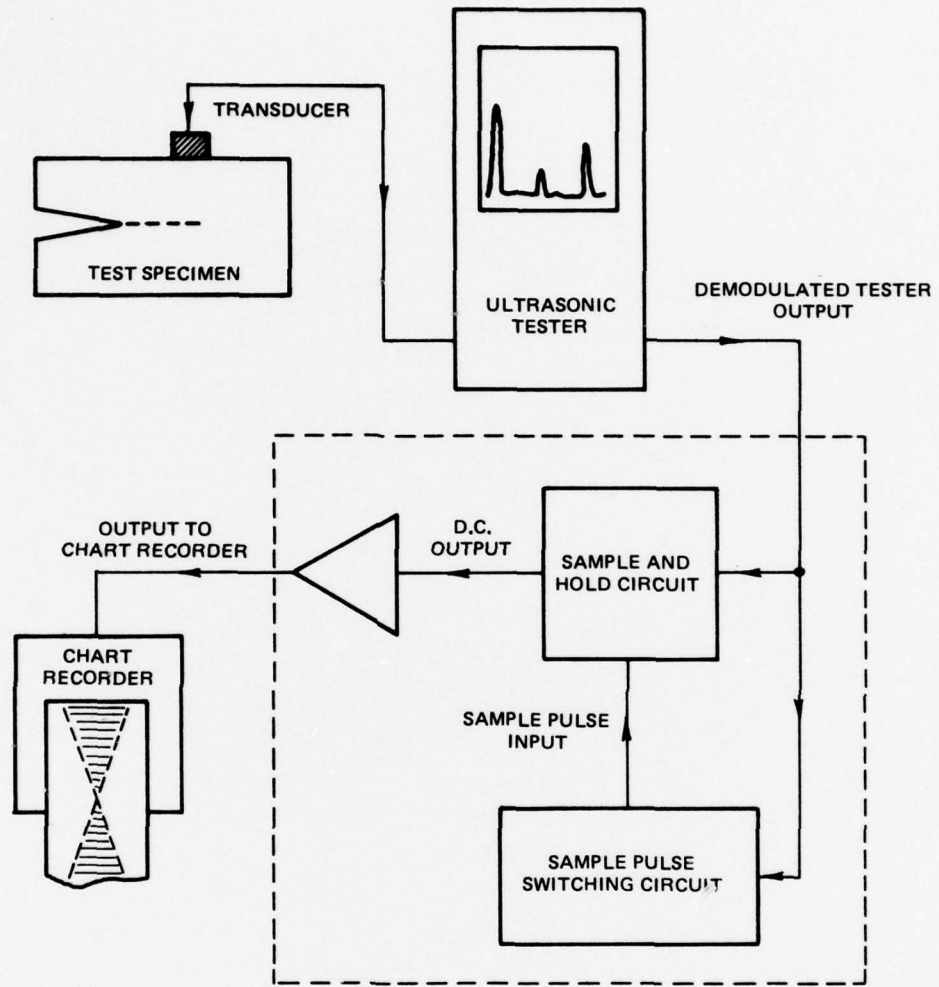


FIG. 4 SIMPLIFIED BLOCK DIAGRAM OF EQUIPMENT USED FOR DIFFERENCE ULTRASONIC CRACK GROWTH MEASUREMENT

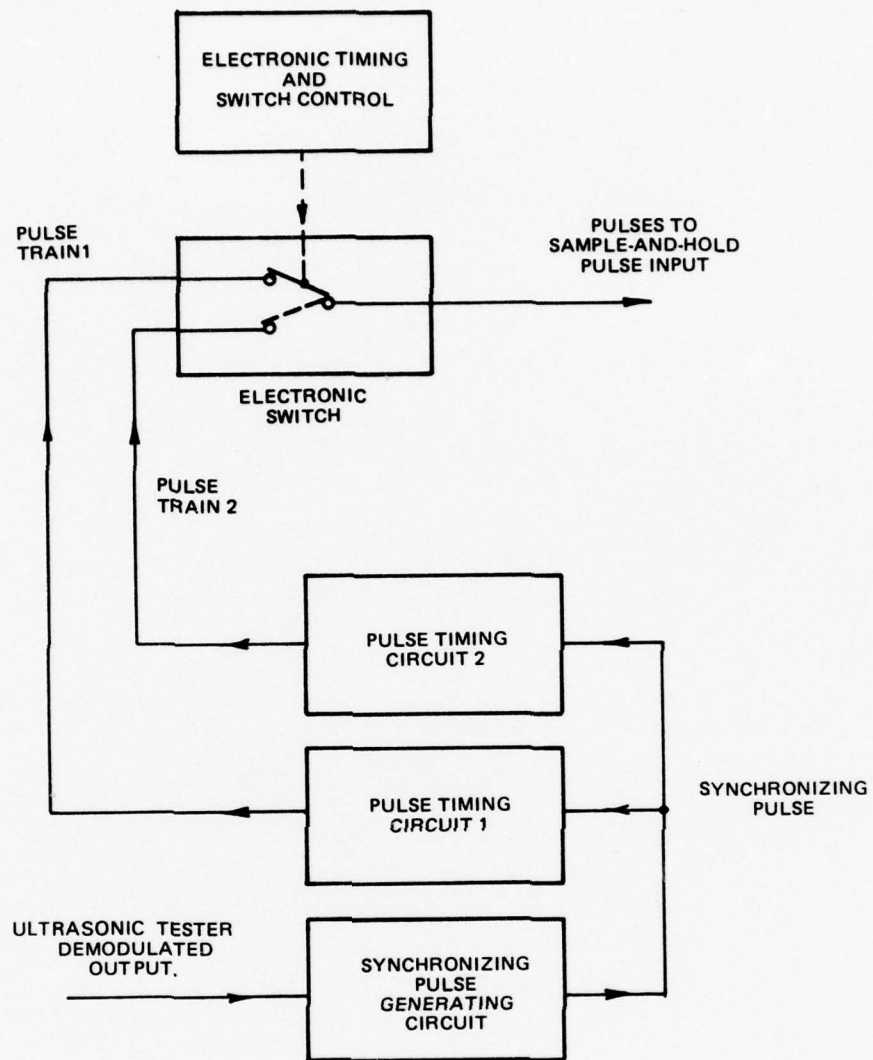


FIG. 5 SIMPLIFIED BLOCK DIAGRAM OF THE SAMPLE PULSE SWITCHING CIRCUIT.

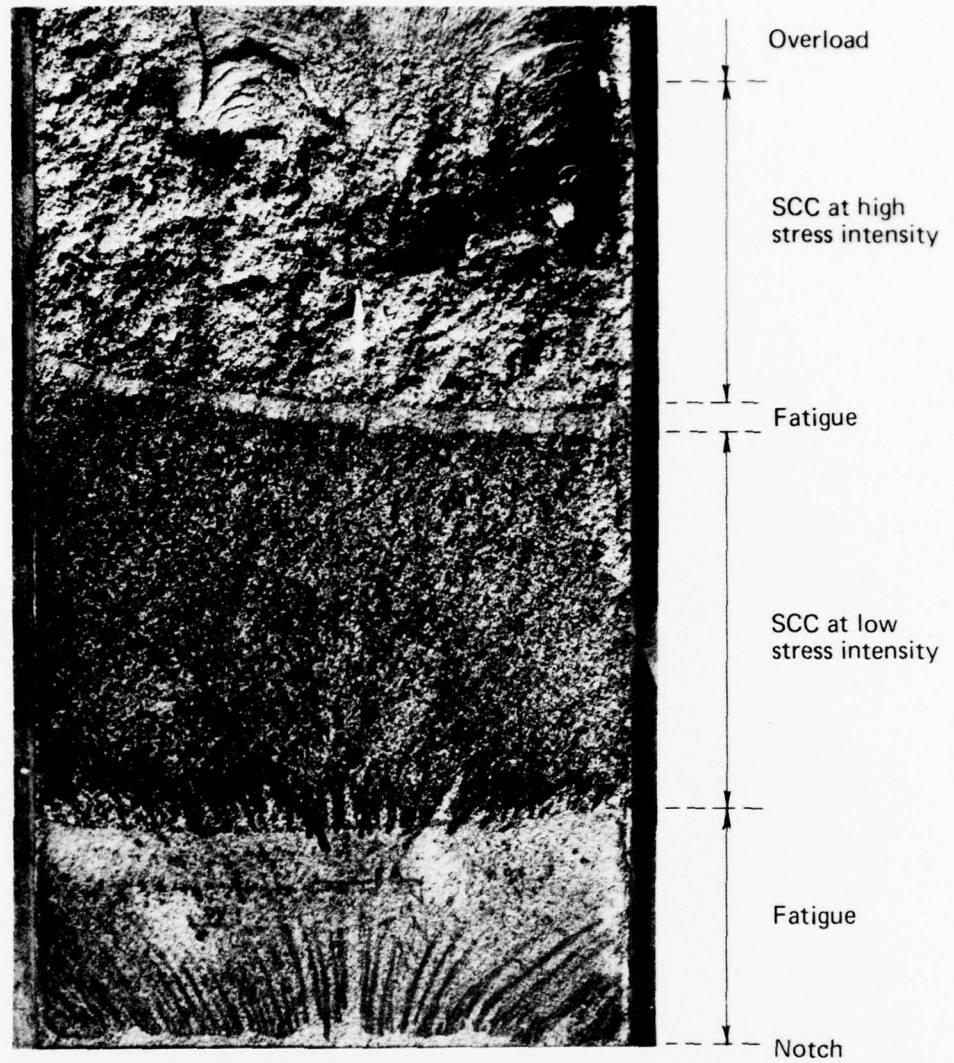
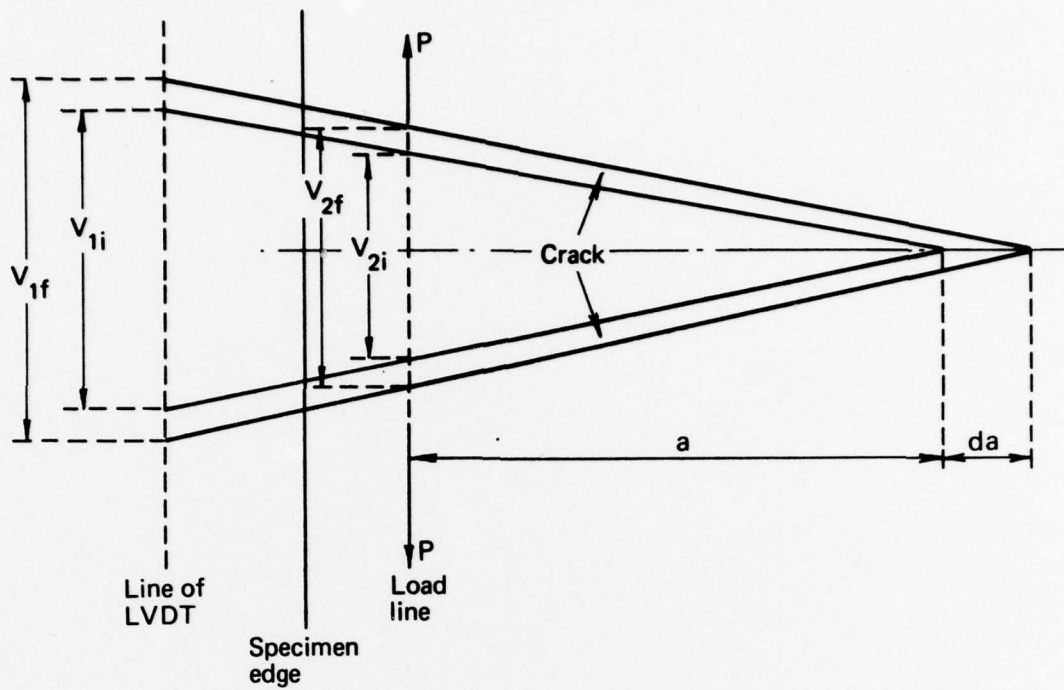


FIG. 6 FRACTURE SURFACE OF D6AC STEEL TEMPERED TO 290°C AND STRESS-CORRODED IN L-T ORIENTATION IN DISTILLED WATER AT 25°C.



a : Crack length from load line

da : Crack extension during SCC

P : Load

V_{1i} : COD at LVDT (load P) for crack of length a

V_{2i} : COD at load line (load P) for crack of length a

V_{1f} : COD at LVDT (load P) for crack of length $a + da$

V_{2f} : COD at load line (load P) for crack of length $a + da$

FIG. 7 SCHEMATIC REPRESENTATION OF CRACK OPENING AT LOAD LINE AND LVDT.

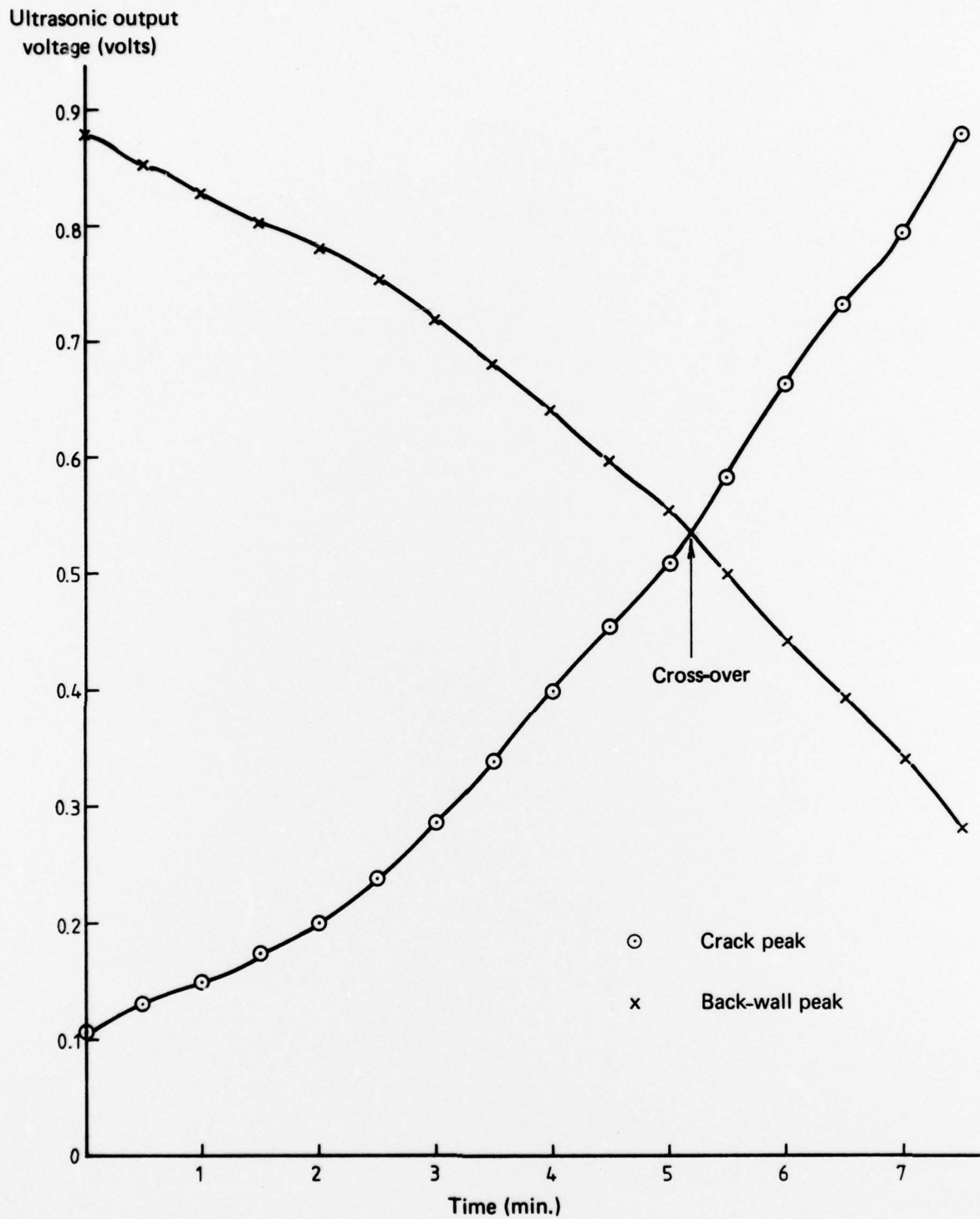


FIG. 8 CHANGE IN AMPLITUDE OF CRACK AND BACK-WALL PEAKS DURING SCC OF D6AC STEEL

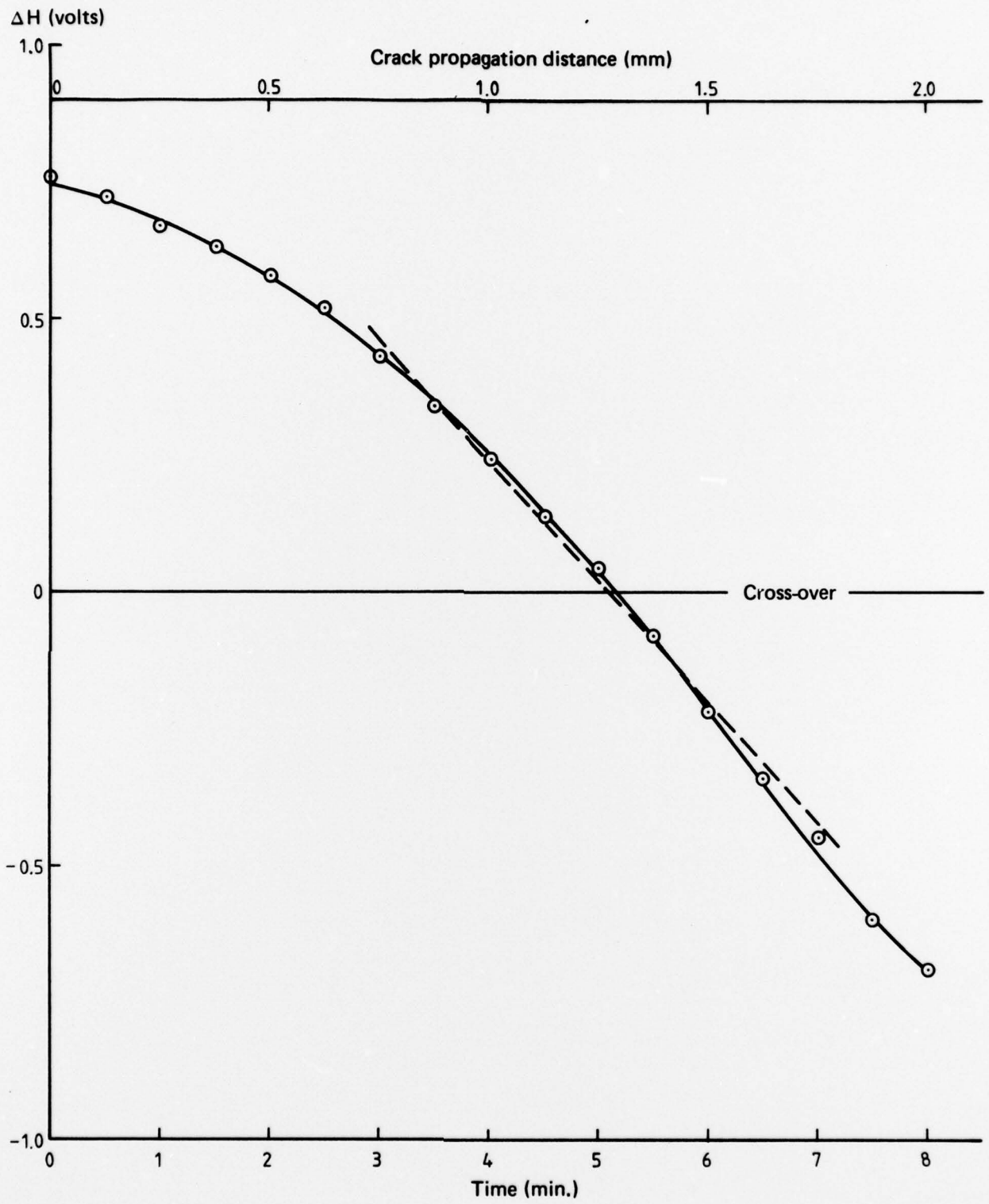


FIG. 9 VARIATION IN ΔH DURING SCC

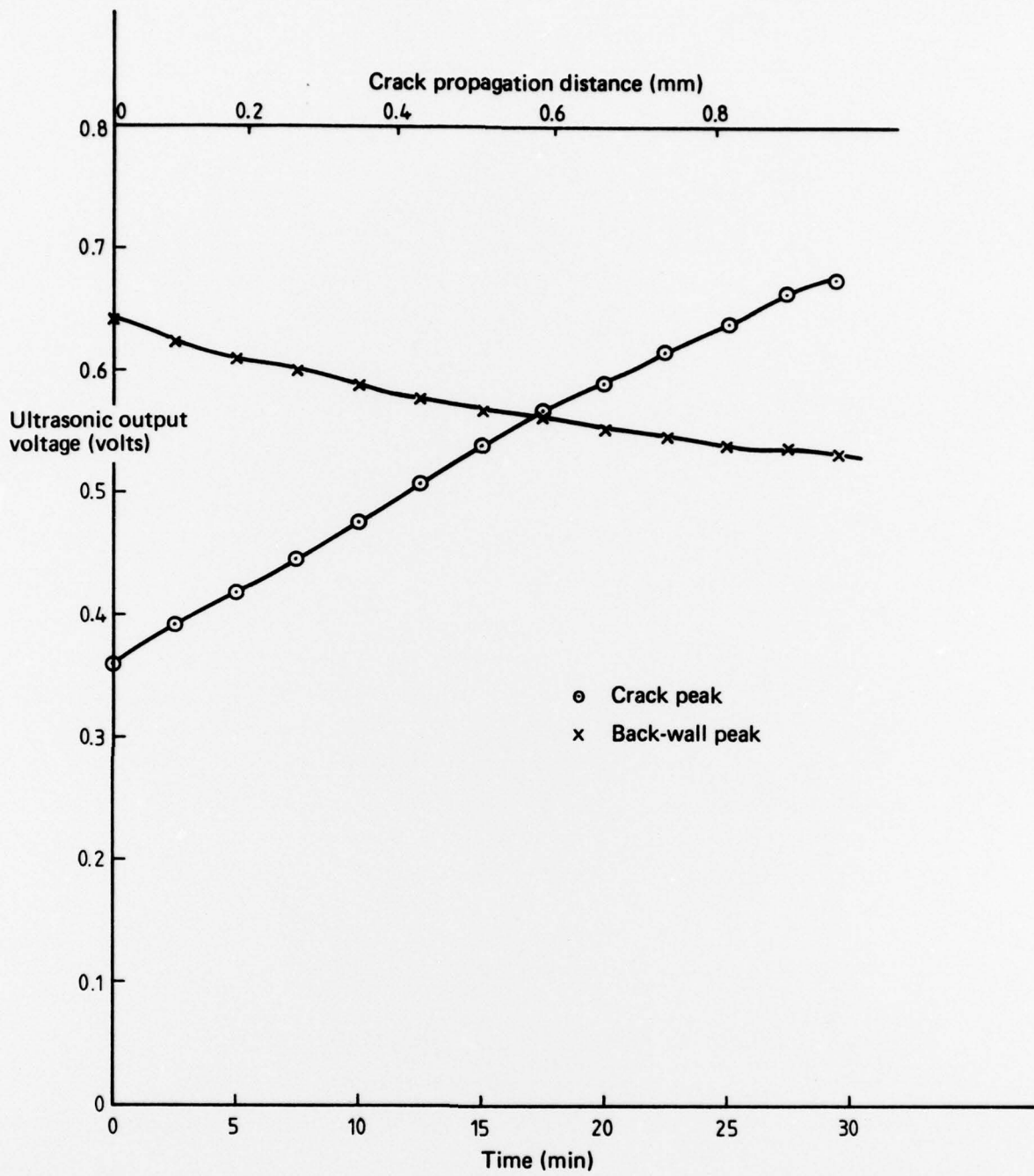


FIG. 10 CHANGE IN AMPLITUDE OF CRACK AND BACK-WALL PEAKS DURING SCC OF D6AC STEEL.

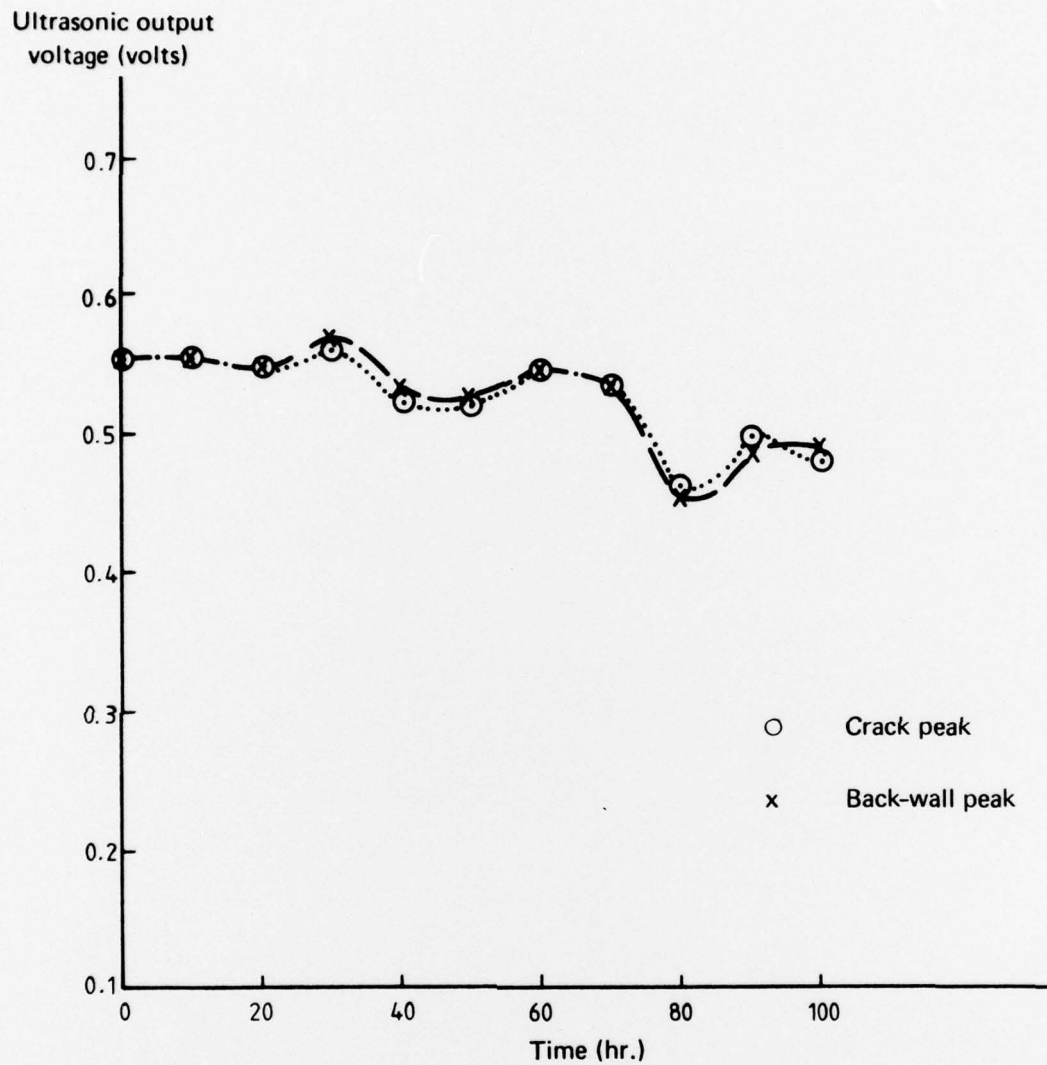


FIG. 11 AMPLITUDE DRIFT OF CRACK AND BACK-WALL PEAKS OF A NON-PROPAGATING CRACK

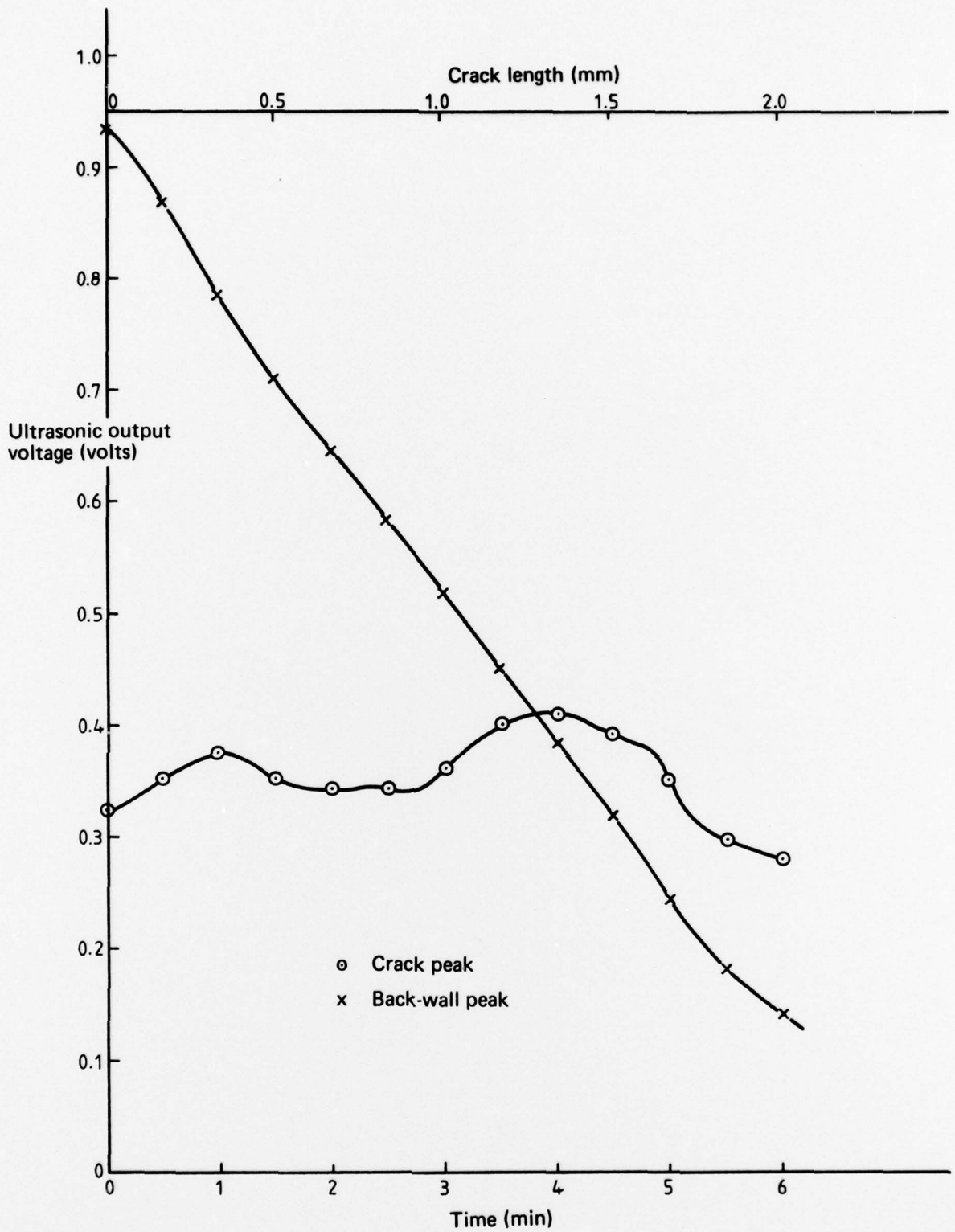


FIG. 12 CHANGE IN AMPLITUDE OF CRACK AND BACK-WALL PEAKS DURING SCC WHICH PRODUCES VERY ROUGH FRACTURE SURFACE.

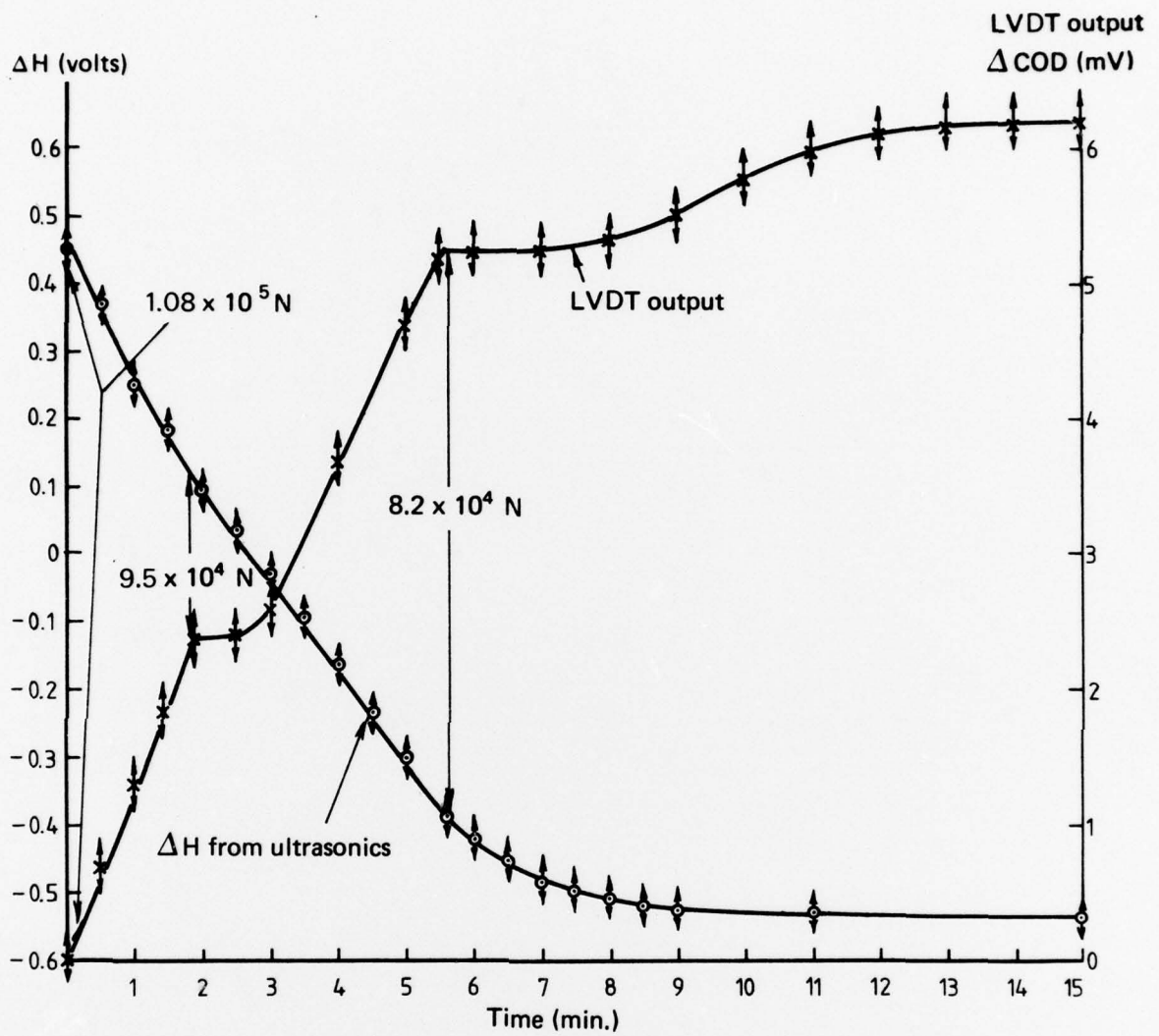


FIG. 13 COMPARISON OF LVDT AND ULTRASONIC DATA AFTER A LOAD REDUCTION

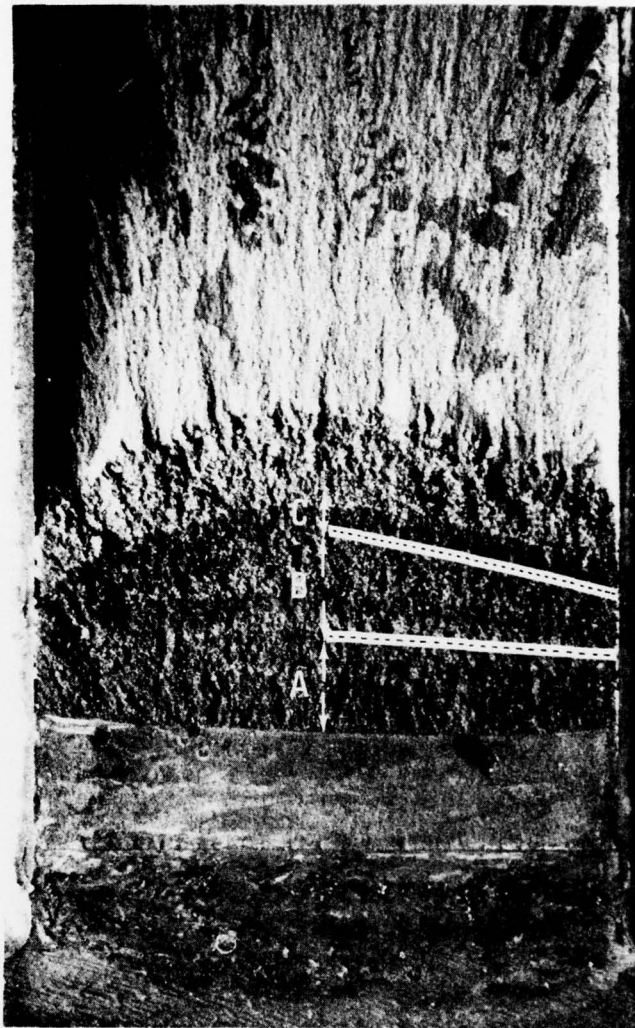


FIG. 14 FRACTURE SURFACE OF D6AC STEEL TEMPERED TO 565°C AND STRESS-CORRODED IN L-T ORIENTATION IN DISTILLED WATER AT 25°C.

A : Region of cracking monitored by first ultrasonic probe.

B : Region of cracking monitored by second ultrasonic probe.

C : Region of cracking monitored by third ultrasonic probe.

..... Oxidation markings on fracture surface outlining crack at various stages of cracking.

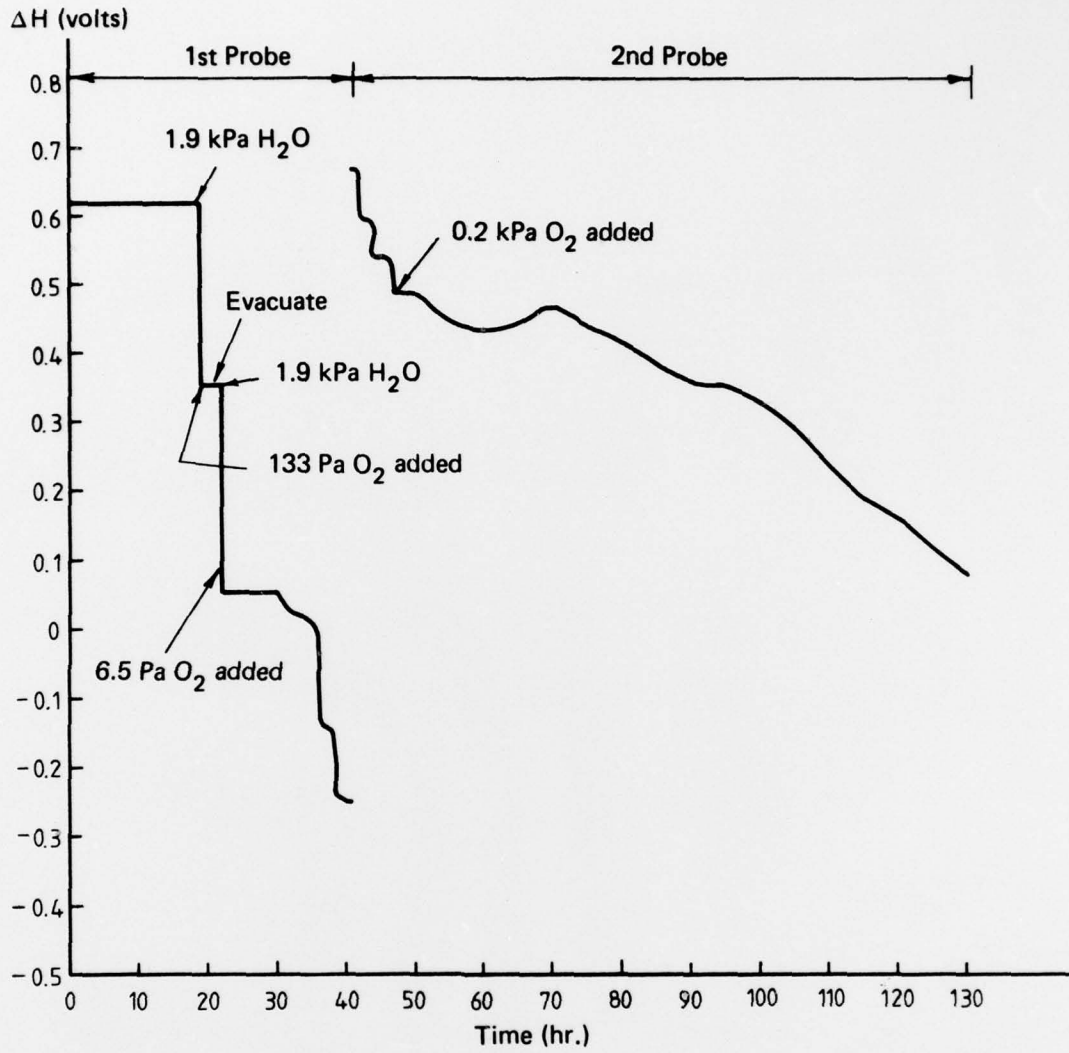


FIG. 15 ULTRASONIC OUTPUT DURING CRACK GROWTH OF D6AC STEEL IN WATER VAPOUR AND WATER-VAPOUR/OXYGEN MIXTURES

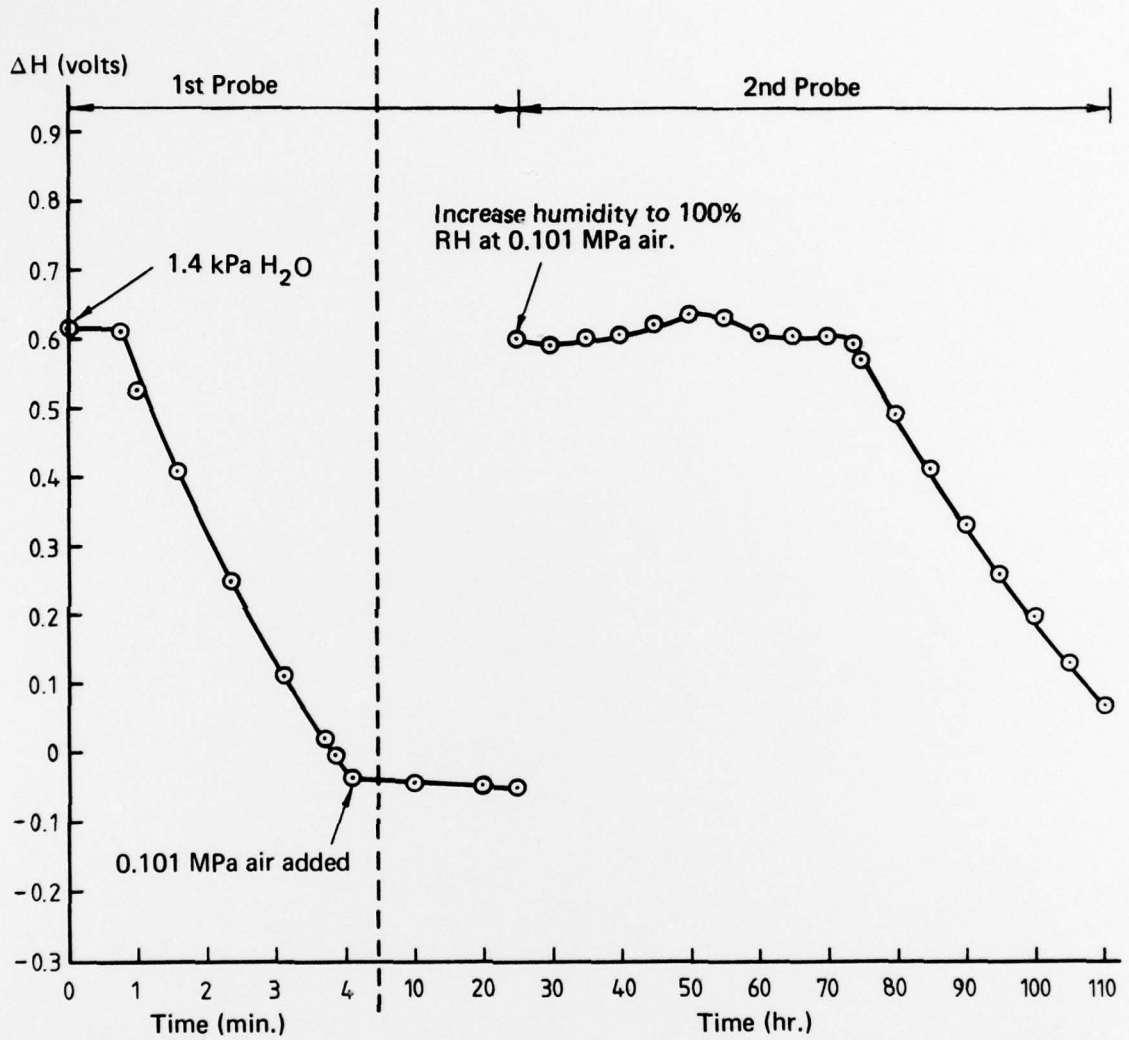


FIG. 16 ULTRASONIC OUTPUT DURING CRACK GROWTH OF SD19 STEEL IN WATER VAPOUR AND 100% RH AIR

DISTRIBUTION

Copy No.

AUSTRALIA

DEPARTMENT OF DEFENCE

Central Office

Chief Defence Scientist	1
Executive Controller, ADSS	2
Superintendent, Defence Science Administration	3
Defence Library	4
JIO	5
Assistant Secretary, DISB	6-21

Aeronautical Research Laboratories

Chief Superintendent	22
Superintendent, Materials	23
Divisional File, Materials	24
W. J. Pollock } Authors	25
A. J. Farrell }	26
Library	27

Materials Research Laboratories

Library	28
---------	----

Weapons Research Establishment

Library	29
---------	----

Central Studies Establishment

Library	30
---------	----

Engineering Development Establishment

Library	31
---------	----

RAN Research Laboratory

Library	32
---------	----

Air Office

Air Force Scientific Adviser	33
Engineering (CAFTS) Library	34
D.Air Eng.	35
H.Q. Support Command (SENGSO)	36

Army Office

Army Scientific Adviser	37
Royal Military College	38
US Army Standardisation Group	39

Navy Office

Naval Scientific Adviser	40
--------------------------	----

DEPARTMENT OF PRODUCTIVITY

Government Aircraft Factories

Library	41
---------	----

DEPARTMENT OF TRANSPORT

Director-General/Library	42
Airworthiness Group (Mr. R. Ferrari)	43

STATUTORY, STATE AUTHORITIES AND INDUSTRY

Australian Atomic Energy Commission (Director) NSW	44
C.S.I.R.O. Central Library	45
C.S.I.R.O. Mechanical Engineering Division (Chief)	46
C.S.I.R.O. Tribophysics Division (Director)	47
Qantas, Library	48
Trans-Australia Airlines, Library	49
S.E.C. Herman Research Laboratory (Librarian) Vic.	50
S.E.C. of Queensland	51
Ansett Airlines of Australia, Library	52
BHP Central Research Laboratories, NSW	53
BHP Melbourne Research Laboratories	54
Commonwealth Aircraft Corporation (Manager)	55
Commonwealth Aircraft Corporation (Manager of Engineering)	56
Hawker de Havilland Pty. Ltd. (Librarian) Bankstown	57
Hawker de Havilland Pty. Ltd. (Manager) Lidcombe	58
Rolls Royce of Australia Pty. Ltd. (Mr. Mosley)	59

UNIVERSITIES AND COLLEGES

Adelaide	Barr Smith Library	60
Australian National	Library	61
Flinders	Library	62
James Cook	Library	63
La Trobe	Library	64
Melbourne	Engineering Library	65
Monash	Library	66
	Professor I. J. Polmear, Materials Engineering	67
Newcastle	Library	68
New England	Library	69
New South Wales	Physical Sciences Library	70
Queensland	Library	71
Sydney	Professor G. A. Bird, Aeronautical Engineering	72
Tasmania	Engineering Library	73
Western Australia	Library	74
RMIT	Library	75
	Mr. Millicer, Aeronautical Engineering	76

CANADA

Aluminium Laboratories Ltd, Library	77
CAARC Co-ordinator Structures	78
NRC, National Aeronautics Est., Library	79

UNIVERSITIES

McGill, Library	80
Toronto Institute of Aerophysics	81

FRANCE

AGARD, Library	82
----------------	----

INDIA		
CAARC Co-ordinator Materials		83
CAARC Co-ordinator Structures		84
Civil Aviation Dept. (Director)		85
Defence Ministry, Aero Development Est., Library		86
Hindustan Aeronautics Ltd, Library		87
Indian Institute of Science, Library		88
Indian Institute of Technology, Library		89
National Aeronautical Laboratory (Director)		90
ISRAEL		
Technion-Israel Institute of Technology (Professor J. Singer)		91
ITALY		
Associazione Italiana di Aeronautica and Astronica, Professor A. Evla		92
JAPAN		
National Aerospace Laboratory, Library		93
UNIVERSITIES		
Tokyo	Institute of Space and Aerospace	94
NETHERLANDS		
Central Organization for Applied Science Research		95
in the Netherlands TNO, Library		96
National Aerospace Laboratory (NLR) Library		97
NEW ZEALAND		
Air Department, R.N.Z.A.F. Aero. Documents Section		98
Transport Ministry, Civil Aviation Division, Library		99
UNIVERSITIES		
Canterbury	Library	100
SWEDEN		
Aeronautical Research Institute		101
SWITZERLAND		
Institute of Aerodynamics E.T.H.		102
Institute of Aerodynamics (Professor J. Ackeret)		103
UNITED KINGDOM		
Australian Defence Science and Technical Representative		104
Aeronautical Research Council		105
C.A.A.R.C., N.P.L. (Secretary)		106
Royal Aircraft Establishment Library, Farnborough		107
Royal Aircraft Establishment Library, Bedford		108
Royal Armament Research and Development Est. Library		109
Aircraft and Armament Experimental Establishment		110
Admiralty Materials Laboratories (Dr. R. G. Watson)		111
National Physical Laboratories, Aero. Division (Superintendent)		112
British Library, Science Reference Library		113
British Library, Lending Division		114
Naval Construction Research Est. (Superintendent)		115
C.A.A.R.C. Co-ordinator, Structures		116
Aircraft Research Association, Library		117

Central Electricity Generating Board		118
Metals Abstracts (Editor)		119
Rolls Royce (1971) Ltd. Aeronautics Division (Chief Librarian)		120
Science Museum Library		121
Welding Institute, Library		122
Welding Institute, Library		122
Hawker Siddeley Aviation Ltd. Brough		123
Hawker Siddeley Aviation Ltd. Greengate		124
Hawker Siddeley Aviation Ltd., Kingston-upon-Thames		125
Hawker Siddeley Dynamics Ltd. Hatfield		126
British Aircraft Corporation (Holdings) Ltd., Commercial Aircraft Div.		127
British Aircraft Corporation (Holdings) Ltd., Military Aircraft		128
British Aircraft Corporation (Holdings) Ltd., Commercial Aviation Div.		129
British Hovercraft Corporation Ltd., (E. Cowes)		130
UNIVERSITIES AND COLLEGES		
Bristol	Library, Engineering Dept.	131
Cambridge	Library, Engineering Dept.	132
Nottingham	Library	133
Southampton	Library	134
Strathclyde	Library	135
Cranfield Institute of Technology,	Library	136
Imperial College	The Head	137
UNITED STATES OF AMERICA		
Counsellor, Defence Science		138
NASA Scientific and Technical Information Facility		139
Sandia Group (Research Organisation)		140
American Institute of Aeronautics and Astronautics		141
The Chemical Abstracts Service		142
Boeing Co. Head Office		143
Boeing Co. Industrial Production Division		144
Cessna Aircraft Co. (Mr. D. W. Mallonée, Executive Engineer)		145
General Electric (Aircraft Engine Group)		146
Lockheed Aircraft Co. (Director)		147
McDonnell Douglas Corporation (Direction)		148
Westinghouse Laboratories (Director)		149
United Aircraft Corporation, Fluid Dynamics Labs.		150
United Aircraft Corporation, Pratt and Whitney Aircraft Division		151
UNIVERSITIES AND COLLEGES		
California	Dr. M. Holt, Department of Aerosciences	152
Cornell (New York)	Library, Aeronautical Labs.	153
Florida	Mark H. Clarkson, Dept. of Aero. Eng.	154
Stanford	Library, Dept. of Aeronautics	155
Brooklyn	Library, Polytech Aeronautical Labs.	156
California	Library, Guggenheim Aero. Labs.	157
Spares		158-167